Demonstration of Laser-Frequency Upshift by Electron-Density Modulations in a Plasma Wakefield

M. Kando,[1] Y. Fukuda,[1] A. S. Pirozhkov,[1,2] J. Ma,[1] I. Daito,[1] L.-M. Chen,[1] T. Zh. Esirkepov,[1,3] K. Ogura,[1] T. Homma,[1] Y. Hayashi,[1] H. Kotaki,[1] A. Sagisaka,[1] M. Mori,[1] J. K. Koga,[1] H. Daido,[1] S. V. Bulanov,[1,3,4] T. Kimura,[1] Y. Kato,[1] and T. Tajima[1]

[1]*Advanced Photon Research Center, JAEA, 8-1 Umemidai, Kizugawa, Kyoto 619-0215, Japan*
[2]*P. N. Lebedev Physical Institute of the Russian Academy of Sciences, Leninsky prospekt 53, 119991 Moscow, Russia*
[3]*Moscow Institute of Physics and Technology, Institutskij pereulok 9, Dolgoprudny, Moscow region 141700, Russia*
[4]*A. M. Prokhorov Institute of General Physics of the Russian Academy of Sciences, Vavilov Street 38, Moscow 119991, Russia*
(Received 16 May 2007; published 24 September 2007)

In a plasma wake wave generated by a high power laser, modulations of the electron density take the shape of paraboloidal dense shells, moving almost at the speed of light. A counterpropagating laser pulse is partially reflected from the shells, acting as relativistic flying mirrors, producing a time-compressed frequency-multiplied pulse due to the double Doppler effect. The counterpropagating laser pulse reflection from the plasma wake wave accompanied by its frequency multiplication (with a factor from 50 to 114) was detected in our experiment.

DOI: 10.1103/PhysRevLett.99.135001 PACS numbers: 52.38.Ph, 52.35.Mw, 52.65.Rr

The development of laser technology [1] has resulted in a tremendous growth in the light intensity in the laser focal spot. Nowadays lasers produce focused irradiance approaching 10^{22} W/cm^2 [2], which makes plasma dynamics ultrarelativistic. By increasing the irradiance further we shall encounter novel physical processes such as the Compton scattering dominated laser-matter interaction [3], and then, at irradiances of the order of 10^{28} W/cm^2 [4], the focused light can generate electron-positron pairs in vacuum, according to [5]. Several ways have been suggested to achieve such intensity [6–8]. Here we consider the ''flying mirror'' concept [6]: dense shells formed in the electron density in a strongly nonlinear plasma wake, generated by a short laser pulse (driver) [9], reflect a portion of a counterpropagating laser pulse (source). The reflected radiation is frequency upshifted, as predicted by Einstein [10], and focused due to the paraboloidal shape of the shells [11,12], caused by the relativistic dependence of the plasma frequency on the wake wave amplitude [13]. This leads to the pulse shortening and light intensification. In this concept the wake wave must be close to wave breaking. If the wake wave is far below the wave-breaking threshold, the reflection is exponentially small. Near the wave-breaking threshold, the reflection becomes much more efficient [6], because the electron density of the shells takes the profile of cusps [13] moving with phase velocity, $v_{\rm ph}$, close to the speed of light c, with the Lorentz factor, γ_e, of electrons forming the shells equal to $\gamma_{\rm ph} = (1 - \beta_{\rm ph}^2)^{-1/2}$, where $\beta_{\rm ph} = v_{\rm ph}/c$. Since the wake wave is generated by the driver pulse, the factor $\gamma_{\rm ph}$ is close to ω_0/ω_p [9], where ω_0 is the laser frequency, $\omega_p = (4\pi n_e e^2/m_e)^{1/2}$ is the plasma frequency, n_e is the electron density, and e and m_e are the electron charge and mass. The frequency of light reflected off the shell at the angle α is upshifted and the pulse duration is shortened by a factor

$$\omega_X(\alpha)/\omega_0 = (1 + \beta_{\rm ph}\cos\theta)/(1 - \beta_{\rm ph}\cos\alpha), \quad (1)$$

where θ is the incidence angle.

The proof-of-principle experiment is performed by colliding two 76 fs laser pulses from the JLITE-X laser at JAEA-Kansai in a helium supersonic gas jet from a 1.26×10 mm^2 nozzle (Fig. 1). The laser produced a 210 mJ, 76 fs driver pulse at a center wavelength of 820 nm, which was focused by an off-axis parabolic mirror in order to make a wake in the supersonic jet. The source pulse, split from the main pulse, was focused to the wake breaking region at the incidence angle $\theta = 45°$ by a plano-convex lens. The driver pulse had a $1/e^2$ focal spot diameter of 27 μm and the estimated irradiance in vacuum of 5×10^{17} W/cm^2. The source pulse energy was 6.3% of the driver pulse, and an estimated irradiance in vacuum of $\approx 10^{17}$ W/cm^2. The fast electrons, generated in the laser-plasma interaction, bent by a permanent magnet, hit a phosphor screen, which was monitored with an intensified CCD. The two laser pulse collision and channeling in the plasma were observed in the shadowgram and interferogram produced by the probe laser beam. The signal reflected by the wake wave was measured with a grazing incidence extreme ultraviolet (XUV) spectrometer composed of a toroidal mirror, a

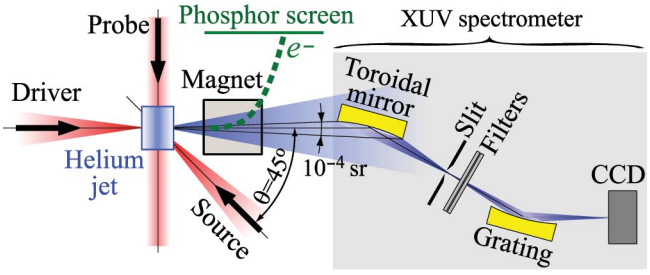

FIG. 1 (color). Setup (top view).

diffraction grating, and a back-illuminated CCD. Two optical filters (freestanding Mo/C multilayer stacks with 60 periods each 2.6 nm thick) were used to block the driver laser light. The spectrometer was calibrated using Ar and Ne emission lines. The spectral resolving power was $\lambda/\Delta\lambda = 100\ (200)$ at 5 nm (15 nm). The spatial resolution in the vertical direction was approximately equal to 60 μm. The acceptance angle was 10^{-4} sr.

To understand the details of the interaction under the present experimental conditions, we performed two-dimensional particle-in-cell (PIC) simulations using the relativistic electromagnetic particle-mesh code [14]. The simulations were carried out for the full-scale plasma and then, with much higher resolution to reveal high frequency upshifts, for the smaller region enclosing the point of intersection of the two pulses. The plasma density and laser irradiance were set according to the conditions of the experiment. In simulations, the driver laser pulse undergoes self-focusing and strong modulation about 300 μm before the gas jet center. As a result, it excites a wakefield with a regular structure, yet close to wave breaking, in a region 200–300 μm before the gas jet center and forms solitons near the jet center. The collision of the two laser pulses is shown in Fig. 2, where the electron-density n_e is normalized to the critical density $n_{cr} = m_e\omega_0^2/4\pi e^2$, the laser pulse fields are in terms of the dimensionless amplitude, $a = eE/m_e\omega_0 c$, and spatial coordinate is in laser wavelengths. The driver pulse excites a wakefield near the wave breaking; the dense shells acting as flying mirrors partially reflect the incident source pulse, whose frequency is anisotropically upshifted due to the mirror curvature. For an ideal reflection of a plane wave the frequency multiplication factor is described by Eq. (1), which defines an ellipse in coordinates (k_x, k_y). This ellipse is shown for $\gamma_{ph} = 4.17$ in Fig. 2(c), where the point (k_x, k_y) corresponds to the spectral intensity of radiation emitted at the angle $\alpha = \arctan(k_y/k_x)$ with frequency $\omega_X(\alpha) = c(k_x^2 + k_y^2)^{1/2}$. The reflected emission at $\alpha = 0$ is estimated as 5.2×10^{10} photons/sr, in agreement with the theoretical prediction.

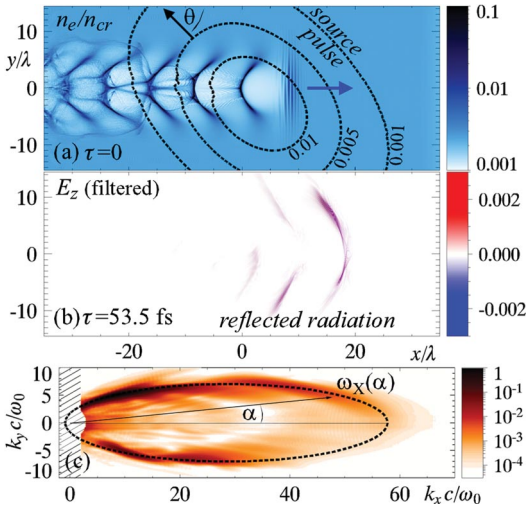

FIG. 2 (color). (a) The electron density disturbed by the driver laser pulse and contours of the source pulse dimensionless amplitude (dashed curves). (b) The reflected radiation seen in the electric field component E_z with frequencies $\leq \omega_0$ filtered out. (c) The reflected radiation spectral intensity; the hatched region is filtered out. The dashed ellipse is for the dependence given by Eq. (1) for $\gamma_{ph} = 4.17$.

Under the experiment conditions the theoretical frequency multiplication factor at $\alpha = 0$ is $\omega_X/\omega_0 \approx 3.4\gamma_{ph}^2$. The plasma density is about 5×10^{19} cm^3. The chosen parameters of the driver pulse and gas jet secure the necessary optimal wake wave excitation, since in previous experiments [15] quasimonoenergetic electron beams were observed under these conditions. We used the fast electron acceleration, of the order of 20 MeV in our case, as evidence of the breaking plasma wake wave formation [16]. Additional evidence of the plasma wave excitation came from the analysis of the scattered driver pulse spectrum observed at 60° (not shown here), which exhibited red- and blueshifted maxima, corresponding to stimulated raman scattering.

In the experiment, it was crucially important to choose the point of the collision of the two laser pulses. Their positions were determined by the shadowgram obtained with the third probe laser beam, as seen in Fig. 3(a). Easing of the source laser pulse aiming onto the wake region was also achieved by observing well localized *stationary spots* inside the self-focusing channel near the center of the gas jet. These spots are seen within the driver path in Fig. 3(b), which is a superposition of two time-integrated images obtained in two shots with different bandpass filters: in one shot the source pulse was alone and the filter window was 414–531 nm, in the other shot the driver pulse was alone and the filter bandwidth was 10 nm at $\lambda = 800$ nm; both pulses could not be seen in one shot since the source pulse was much weaker. According to our simulations,

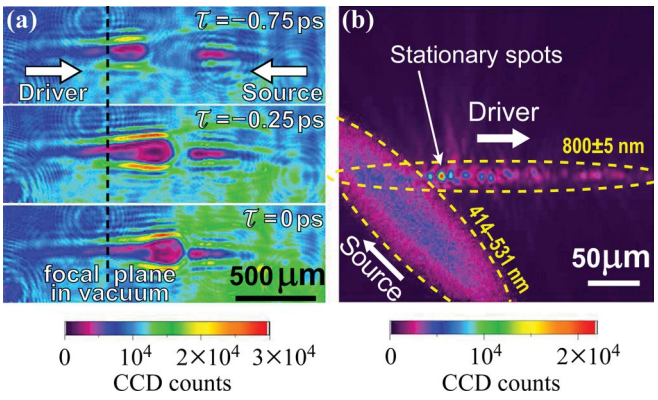

FIG. 3 (color). (a) Side-view shadowgraphs produced by the 76-fs probe beam for different delays between driver and source pulses. (b) Superimposed time-integrated top-view images obtained in two shots, where either the driver pulse or the source pulse was present. Both pulses could not be seen in one shot since the source is much weaker than the driver.

stationary spots were identified as postsolitons, the late stages of the evolution of relativistic electromagnetic solitons [17]. They appear where the laser pulse energy is substantially depleted and thus indicate the limit to which the good quality wake extends.

The temporal overlapping with picosecond accuracy was controlled by an analysis of the transmitted source spectrum. The blueshift caused by ionization effects [18] was observed irrespective of the driver pulse presence. However, a delay-dependent additional blueshift was observed when the source pulse intersected the wake wave region, due to the fast change of the refractive index there. An accuracy of a few microns times tens femtoseconds was required to point the source laser pulse at the location of the wake wave breaking, where the flying mirror is formed. This was met by observing a *moving spot* in the scattered light of the unfocused source pulse; Fig. 4. In contrast to *stationary spots*, also seen in Fig. 3(b), the position of this 15–20 μm spot, x_{ms}, changes monotonically with decreasing time delay between the pulses. The *moving spot* is interpreted as the electron-density modulation, associated with the driver pulse and a wake region behind it, leading to the source pulse refraction. Since the driver pulse propagates at $\theta = 45^{\circ}$ with respect to the monitor object plane, the corresponding image velocity is $v_{\mathrm{ms}} = c\sin\theta/(1 + \cos\theta) \approx 0.414c$, in agreement with the observed velocity $(0.416 \pm 0.003)c$ of the *moving spot*, Fig. 4. Aiming at the *moving spot*, we varied the delay time between pulses, τ, and the vertical position, z, of the source pulse. In this way a wide range of colliding point coordinates was scanned.

We detected 24 signals of the reflected radiation in 24 different shots. In Fig. 5, each point represents the photon number, corresponding to the peak of the spectrum extracted from a readout of the XUV spectrometer CCD in a single shot, as in Fig. 6. We note that the reflectivity of the electron-density shell can be smaller at greater gamma factors [6]. The XUV spectrometer has the spectral range of 4–18 nm, which is narrowed by the filter absorption to 5–15 nm. The signals occurred within 7–15 nm. A majority of the signals was seen when the colliding point was

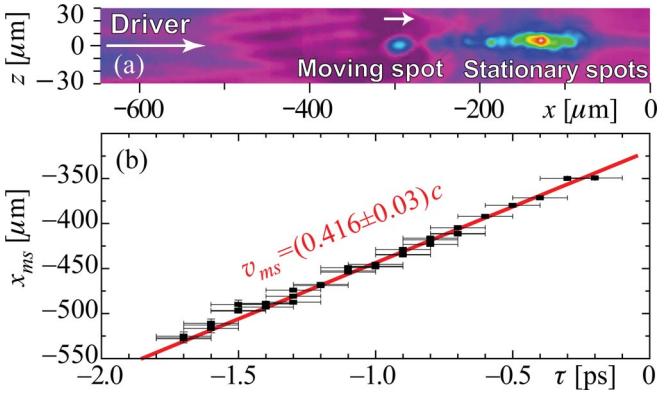

FIG. 4 (color). (a) The side-view shadowgraph produced by an unfocused source pulse. (b) Moving spot position, x_{ms}, vs time delay, τ, between the driver and the source pulses.

located 200 μm before the gas jet center (the driver focal plane was located 600 μm before the gas jet center). As seen in Fig. 5 (inset), the detected photon number correlates with the accuracy of targeting, imposing constraints on the vertical size of the flying mirror and the duration of the incident radiation (before reflection), in agreement with the expected wake wave transverse size and the source pulse duration.

Figure 6 shows the spectrum extracted from the XUV spectrometer readout, where the signal corresponds to the peak at the wavelength $\lambda_X = 14.3$ nm, which is 56 times shorter than the incident source pulse wavelength. The detected spectral peak (60 counts) is more than 5 times higher than the noise level ($\sigma = 12$ counts). The signal bandwidth is $\Delta\lambda_X = 0.3$ nm and the detected photon number per shot is $N_d = 25 \pm 7$. The uncertainty in the photon number arises from both the shot noise and the background emission. Using idealized values for the spectrometer toroidal mirror reflectivity $R_T = 0.8$, the transmission of two filters $T_F = 0.3^2$, the diffraction grating efficiency $\eta_G = 0.2$ and the CCD quantum efficiency $\eta_{\mathrm{CCD}} = 0.4$, we can estimate the number of photons produced by the relativistic flying mirror formed in the plasma wake wave. Taking into account the spectrometer acceptance angle (10^{-4} rad), we find the emission of 3×10^7 photons/sr. This number is lower than the theoretically estimated value and the number seen in the PIC simulations because of the nonoptimal conditions of the collision. Not taken into account here are the effects of contamination, spectrometer optics roughness, source pulse attenuation, etc., which can substantially increase the estimated number of reflected photons.

The detected wavelength 14.3 nm and shortening factor $\lambda_0/\lambda_X \approx 3.4\gamma_{\mathrm{ph}}^2$ (due to reflection from the flying mirror) give a Lorentz factor of $\gamma_{\mathrm{ph}} = 4.1$. We can also estimate

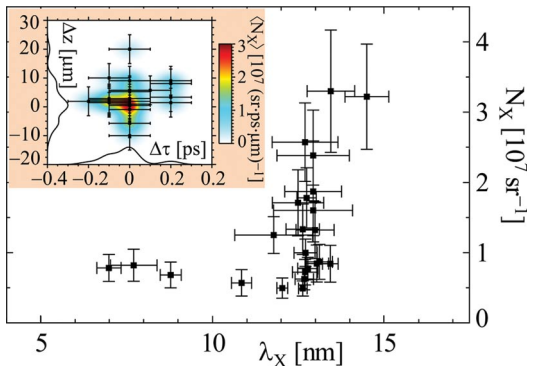

FIG. 5 (color). XUV signals. Each point corresponds to the peak of a spectrum obtained in a single shot (the background is subtracted), as in Fig. 6. Horizontal and vertical bars are for the spectral width and the photon number uncertainty, respectively. Inset: the same signals arranged in the plane $(\Delta\tau, \Delta z)$, where $\Delta\tau$ and Δz correspond to the targeting in time and space. The photon number density is obtained by attributing a Gaussian distribution to each point, with FWHM widths determined by the resolution of the monitors.

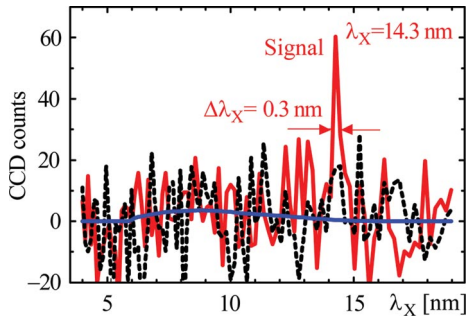

FIG. 6 (color). The spectrum of the signal at 14.3 nm (solid line) and a typical spectrum obtained without the source pulse (dashed line); the background is subtracted in both cases. The blue line is for calculated Thomson scattering (see text).

this factor from the fast electron bunch energy, $\mathcal{E}_b = m_e c^2 \gamma_b \approx 2 m_e c^2 \gamma_{\rm ph}^2$ [9]. From the 19 MeV electrons detected in this shot (see also [15], where the electron acceleration was detected under the same conditions), we obtain $\gamma_{\rm ph} = 4.3$, in good agreement with the previous estimation. An assumption that the reflected signal has inherited the coherence from the source pulse, yields its estimated duration to be 1.4 fs, consistent with the observed spectral width $\Delta\lambda_X/\lambda_X \approx 1/48$. Our simulations also match well with the spectral characteristics such as the value of $\gamma_{\rm ph}$, λ_X, and $\mathcal{E}_b$.

Without the source pulse, we observed a background emission from a region with vertical size equal to 200–300 μm. This background included a continuous bremsstrahlung plasma emission. The detected signal represents an emission from a much more localized region. The XUV spectrometer spatial resolution gave an upper limit of 60 μm for the signal vertical size. As seen in the inset in Fig. 5, the signal origin localization was much tighter, of the order of 10 μm. Since the signal appeared only when the source pulse is present and was isolated both in space-time (Fig. 5, inset) and in the spectral distribution (Fig. 6), it cannot be explained by high-order harmonics generated as a result of nonlinear polarization of atoms [19] in the driver pulse or its spatial wings or due to relativistic effects [20], though these harmonics can contribute to the background. The narrow bandwidth of the detected signals hinders explaining the reflection in terms of Thomson scattering. Figure 6 shows an upper limit for the signal due to Thomson scattering from a single density cusp, calculated in a one-dimensional model of a nonlinear wake wave [13] with a parabolic dependence of the wakefield maximum gamma factor, γ_m, on the distance from the axis r: $\gamma_m = \gamma_{\rm ph}[1 - r^2/(2r_0^2)]$, where $r_0 \approx 2$ μm is taken from the PIC simulation. This signal spectral width is ≈ 5 nm $\gg \Delta\lambda_X$. The contribution from the Thomson scattering off fast electrons is orders of magnitude smaller than the detected photon number within the given spectral range and its spectrum is much broader [21]. For the detected signals, the reflection off electrons occurs in a collective manner mainly at dense shells in the electron density, as described in the flying mirror concept [6].

In conclusion, our measurements and supporting simulations may evidence the first observation of a collective relativistic frequency multiplier through two colliding laser pulses in plasma. This gives the proof-of-principle of the flying mirror concept. The observed XUV signal can also help to measure the wake wave phase velocity, spatial profile, and duration, which is a challenging problem requiring femtosecond time resolution [12]. According to theoretical estimations [6,8], in the future the flying mirror concept will hopefully allow the production of tunable sources of hard electromagnetic radiation with controlled parameters desired for a wide range of applications [8,22].

This work was supported by the Ministry of Education, Science, Sports and Culture of Japan, Grant-in-Aid for Specially Promoted Research No. 15002013.

[1] D. Strickland and G. Mourou, Opt. Commun. **56**, 219 (1985).
[2] S.-W. Bahk *et al.*, Opt. Lett. **29**, 2837 (2004).
[3] A. G. Zhidkov *et al.*, Phys. Rev. Lett. **88**, 185002 (2002); S. V. Bulanov *et al.*, Plasma Phys. Rep. **30**, 196 (2004).
[4] N. B. Narozhny *et al.*, Phys. Lett. A **330**, 1 (2004).
[5] W. Heisenberg and H. Euler, Z. Phys. A **98**, 714 (1936); J. Schwinger, Phys. Rev. **82**, 664 (1951).
[6] S. V. Bulanov *et al.*, Phys. Rev. Lett. **91**, 085001 (2003).
[7] N. M. Naumova *et al.*, Phys. Rev. Lett. **92**, 063902 (2004); S. Gordienko *et al.*, *ibid.* **94**, 103903 (2005).
[8] G. Mourou *et al.*, Rev. Mod. Phys. **78**, 309 (2006).
[9] T. Tajima and J. M. Dawson, Phys. Rev. Lett. **43**, 267 (1979).
[10] A. Einstein, Ann. Phys. (Leipzig) **17**, 891 (1905).
[11] S. V. Bulanov and A. S. Sakharov, JETP Lett. **54**, 203 (1991).
[12] N. H. Matlis *et al.*, Nature Phys. **2**, 749 (2006).
[13] A. I. Akhiezer and R. V. Polovin, Sov. Phys. JETP **3**, 696 (1956).
[14] T. Zh. Esirkepov, Comput. Phys. Commun. **135**, 144 (2001).
[15] M. Mori *et al.*, Phys. Lett. A **356**, 146 (2006).
[16] S. P. D. Mangles *et al.*, Nature (London) **431**, 535 (2004); C. Geddes *et al.*, Nature (London) **431**, 538 (2004); J. Faure *et al.*, Nature (London) **431**, 541 (2004); A. Yamazaki *et al.*, Phys. Plasmas **12**, 093101 (2005); B. Hidding *et al.*, Phys. Rev. Lett. **96**, 105004 (2006); W. Leemans *et al.*, Nature Phys. **2**, 696 (2006).
[17] N. M. Naumova *et al.*, Phys. Rev. Lett. **87**, 185004 (2001); M. Borghesi *et al.*, *ibid.* **88**, 135002 (2002); L.-M. Chen *et al.*, Phys. Plasmas **14**, 040703 (2007).
[18] W. M. Wood *et al.*, Opt. Lett. **13**, 984 (1988); J. K. Koga *et al.*, Phys. Plasmas **7**, 5223 (2000).
[19] J. G. Eden, Prog. Quantum Electron. **28**, 197 (2004).
[20] S.-Y. Chen *et al.*, Nature (London) **396**, 653 (1998).
[21] H. Schwoerer *et al.*, Phys. Rev. Lett. **96**, 014802 (2006).
[22] V. Malka *et al.*, Plasma Phys. Controlled Fusion **47**, B481 (2005).